Author Manuscript

Author Manuscript

Author Manuscript

Author Manuscript

HHS Public Access

Author manuscript

Acta Biomater. Author manuscript; available in PMC 2020 November 01.

Published in final edited form as:

Acta Biomater. 2019 November ; 99: 72–83. doi:10.1016/j.actbio.2019.08.032.

A Superoxide Scavenging Coating for Improving Tissue Response to Neural Implants

X. Sally Zheng[a,*], **Noah R. Snyder**[a,c,*], **Kevin Woeppel**[a,b,*], **Jenna Hanner**[a], **Xia Li**[a], **James Eles**[a,c], **Christi L. Kolarcik**[a,b,c,d], **X. Tracy Cui**[a,b,c]

[a]Department of Bioengineering, University of Pittsburgh, PA USA

[b]Center for the Neural Basis of Cognition, University of Pittsburgh, PA USA

[c]McGowan Institute for Regenerative Medicine, University of Pittsburgh, PA USA

[d]Systems Neuroscience Institute, University of Pittsburgh, PA USA.

Abstract

The advancement of neural prostheses requires implantable neural electrodes capable of electrically stimulating or recording signals from neurons chronically. Unfortunately, the implantation injury and presence of foreign bodies leads to chronic inflammation, resulting in neuronal death in the vicinity of electrodes. A key mediator of inflammation and neuronal loss are reactive oxygen and nitrogen species (RONS). To mitigate the effect of RONS, a superoxide dismutase mimic compound, manganese(III) meso-tetrakis-(N-(2-aminoethyl)pyridinium-2-yl) porphyrin (iSODm), was synthesized to covalently attach to the neural probe surfaces. This new compound showed high catalytic superoxide scavenging activity. In microglia cell line culture, the iSODm coating effectively reduced superoxid production and altered expression of iNOS, NADPH oxidase, and arginase. After 1 week of implantation, iSODm coated electrodes showed significantly lower expression of markers for oxidative stress immediately adjacent to the electrode surface, as well as significantly less neurons undergoing apoptosis.

Graphical Abstract

One critical challenge in translation of neural electrode technology to clinically viable devices for brain computer interface or deep brain stimulation applications is the chronic degradation of the device performance due to neuronal degeneration around the implants. One of the key mediators of inflammation and neuronal degeneration is reactive oxygen and nitrogen species released by injured neurons and inflammatory microglia. This research takes a biomimetic approach to synthesize a compound having similar reactivity as superoxide dismutase, which can catalytically

Corresponding author: X. Tracy Cui, Ph.D., Department of Bioengineering, University of Pittsburgh, 5057 Biomedical Science Tower 3, 3501 Fifth Avenue, Pittsburgh, PA 15260, Ph: 412-383-6672, FAX: 412-648-9076, xic11@pitt.edu.

*:Contributing equally.

7.Disclosure

Noah Snyder, James Eles and Xinyan Cui are inventors of the patent related to the antioxidant coating reported here, and the patent is currently licensed to Interphase Materials. Noah Snyder is currently the CEO of Interphase Materials.

Publisher's Disclaimer: This is a PDF file of an unedited manuscript that has been accepted for publication. As a service to our customers we are providing this early version of the manuscript. The manuscript will undergo copyediting, typesetting, and review of the resulting proof before it is published in its final citable form. Please note that during the production process errors may be discovered which could affect the content, and all legal disclaimers that apply to the journal pertain.

Author Manuscript Author Manuscript Author Manuscript Author Manuscript

scavenge reactive oxygen and nitrogen species, thereby reducing oxidative stress and decrease neuronal degeneration. By immobilizing the compound covalently on the surface of neural implants, we show that the neuronal degeneration and oxidative stress around the implants is significantly reduced.

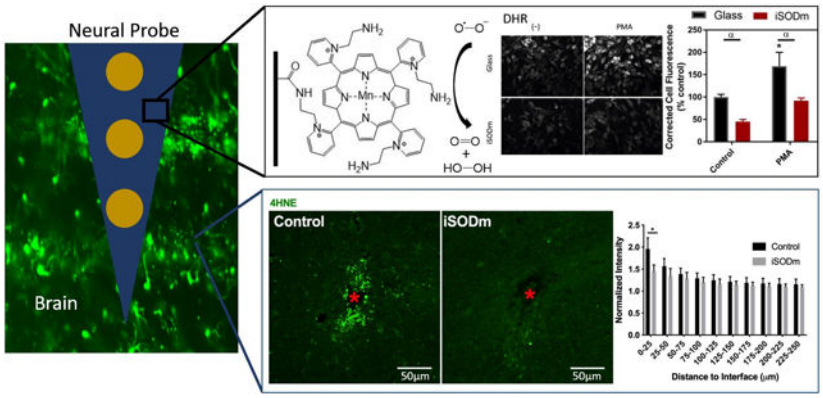

Keywords

reactive oxygen species; inflammation; neuronal degeneration; neural electrodes; chronic neural recording

1.0 Introduction

Neurotechnology has offered new ways to interface with the nervous system. By implanting microelectrodes into neural tissue, extracellular potential changes can be recorded. Conversely, via the application of electrical current, neurons can be excited or inhibited to result in network changes and behavioral modifications. This technology has been the foundation for many neural prosthetic devices which have the potential to restore motor or sensory function to the millions with nervous system injuries or neurodegenerative diseases [1]. However, implant performance is often riddled with host tissue responses such as inflammation and neuronal loss. Within the CNS, microglia/macrophages have been identified to be the primary cell type immediately contacting implanted electrodes after device insertion and throughout the implantation period [2, 3]. Once activated, microglia secrete pro-inflammatory cytokine, initiate the recruitment of additional macrophages/microglia, and produce various cytotoxic factors such as excitatory amino acids and reactive oxygen and nitrogen species (RONS) [4]. Given the proximity of these cells to the neural implants and their activation state, RONS produced nearby may directly result in an environment that promotes neurodegeneration, as in the cases of various neurological disorders [5-10]. In these neurodegenerative disorders, activated microglia produce oxidative stress through the enzymatic production of superoxide and nitric oxide by NADPH oxidase and inducible NO synthase (iNOS), respectively, resulting in neuron death. Furthermore, nearby dying cells activate and recruit more microglia producing a feedforward loop of neuronal death [11-13]. Similarly a reduction of neuron density and the presence of caspase-3 positive neurons [14] and degenerating neuronal processes [15] were observed near the neural implants, which are accompanied with an increase in ROS level [16-18].

Author Manuscript Author Manuscript Author Manuscript Author Manuscript

Additionally, ROS may accelerate the degradation of intracortical microelectrodes [18, 19], which could lead to poor chronic functionality. Therefore, strategies aiming at controlling ROS at the vicinity of the implanted neural electrodes need to be developed for the high quality and longevity of neural interfacing. One strategy to control ROS is via administration of an antioxidant, which has shown promising effects in reducing neuronal loss around the implanted device [17, 20, 21]. However, systemic administration brings the risk of side effects [17] while the local delivery of antioxidant needs to overcome the limitation on drug loading capacity[22].

The level of oxidative stress is typically held in balance by the superoxide dismutase (SOD) enzyme family, which can remove superoxide through a process that converts the radical to molecular oxygen and hydrogen peroxide. However, using SOD directly to treat diseases influenced by oxidative stress, including neurodegenerative diseases, has been largely unsuccessful due to low stability, poor bioavailability, immunogenicity, and other negative factors [23, 24]. In recent years, the development of low molecular weight synthetic molecules that mimic the function of SOD has provided potential pharmaceutical agents for treating oxidative stress [23-26]. One SOD mimic (SODm) in particular, manganese(III) meso-tetrakis-(N-ethylpyridinium-2-yl) porphyrin (Mn^{III}TE-2-Pyp5+), has proven to be neuroprotective in *in vitro* models of Alzheimer's disease [27] as well as in *in vivo* models of stroke [28]. Furthermore, Mn^{III}TE-2-Pyp5+ is an equally capable peroxynitrite scavenger, a byproduct of the superoxide and nitric oxide released by microglia, making it an ideal compound for reducing a variety of RONS produced in the context of neurological disorders [23-25]. To reduce the oxidative stress and improve the neuronal survival near chronically implanted neural electrodes, we designed a new coating based on a synthetic derivative of Mn^{III}TE-2-$Pyp5^{+}$, iSODm (immobilizable SODm). Due to the catalytic nature of the molecule, the antioxidant effect may be regenerated indefinitely, which is advantageous over the drug elution strategy. Here, we describe the synthesis and coating strategy of iSODm, *in vitro* characterization of the SODm coating, and *in vivo* histological evidence demonstrating a reduction in oxidative stress and improvement in neuronal health near iSODm-coated neural electrodes.

2.0 Materials and Methods

2.1 Chemicals and Reagents

The unsubstituted porphyrin, H_2T-2-Pyp, as well as the metalloporphyrin, Mn^{III}TE-2-Pyp5+ (manganese(III)-5,10,15,20-tetrakis(N-ethylpyridinium-2-yl)porphyrin) herein referred to as SODm, was purchased from Frontier Scientific, Inc. (Logan, UT). Resveratrol as well as manganese (III) tetrakis (4-benzoic acid) porphyrin chloride (MnTBAP) were purchased from EMD Millipore Corp. (Billerica, MA). The remaining chemical reagents, biological reagents, and solvents were purchased from Sigma Aldrich (St. Louis, MO).

2.2 Synthesis of the *Immobilizable Superoxide Dismutase Mimic* (iSODm)

The preparation of the alkylamine functionalized metalloporphyrin, MnIIITEA-2-Pyp5+ (manganese(III)-5,10,15,20- tetrakis(N-(2-aminoethyl)pyridinium-2-yl)porphyrin) herein referred to as iSODm, occurs via a one-pot synthesis and direct metalation of the

Author Manuscript Author Manuscript Author Manuscript Author Manuscript

unsubstituted porphyrin H_2T-2-Pyp (meso-Tetra (2-pyridyl) porphine) (Scheme 1), similar to synthesis by Kos et. al. [29]. The unsubstituted porphyrin, H_2T-2-Pyp, was dissolved in dimethylformamide (DMF) with excess 2-bromethylamine (BEA). The temperature was raised to 100 °C and the reaction was kept under reflux for 24 – 48 hours. The extent of the reaction was measured via the progressive appearance of mono-, di-, tri-, and tetra-substituted porphyrin species monitored via thin-layer chromatography (TLC) with a mobile phase of H_2O, acetonitrile, and saturated $K(NO_3)$ in H_2O at 8:1:1 concentration. A sample of the resulting modified porphyrin was isolated from a silica packed column with the same 8:1:1 mobile phase. Validation of modified porphyrin was performed with 1H NMR at 400MHz. While the reaction was not expected to and did not proceed to completion, the formation of amine-bound arms was confirmed by the formation of peaks at 4.5ppm and 3.02 ppm corresponding to hydrogens bound to carbons adjacent to the pyridinium and amine, respectively. Further, an upstream shift of the pyridinium peaks was noted.

Following completion of the reaction to the tetra- substituted porphyrin, excess $MnCl_2$ was added directly to the flask and the reaction was kept under reflux for an additional 24 – 48 hours. The progression of the reaction was monitored by observation of the Soret band after metalation shift to 450 nm. After the completion of the reaction, the solution was cooled to room temperature and the final metalloporphyrin product was precipitated by the addition of tetrahydrofuran (THF). The water-soluble product was dissolved in water and crystallized using a saturated ammonium hexafluorophosphate solution. The final product was prepared by dissolving the hexafluorophosphate salt complex in acetone and precipitation with tetrabutylammonium chloride. Secondary validation of the structure was performed with Fourier Transform Infrared Spectroscopy (FTIR), confirming the presence of amine-terminated groups and aliphatic carbon chains which are not present on the precursor porphyrin (Fig. S1).

2.3 Electrochemical Characterization of the iSODm Complex

Electrochemical measurements were performed in a glass cell containing a glassy carbon working electrode (3 mm in diameter), a Pt foil counter electrode, and an Ag/AgCl reference electrode (in 3 M KCl solution) using the Autolab Potentiostat/Galvanostat (Metrohm). Measurements were taken of 10 mM iSODm in 0.2 mM PBS, pH = 7.5 at a scan rate of 100 mV/s between −0.31 V to 0.29 V vs Ag/AgCl (equivalent of −0.1V to 0.5V vs NHE).

2.4 Superoxide Scavenging Activity of iSODm

To determine the catalytic superoxide scavenging nature of the synthesized iSODm complex in comparison to other antioxidants, the cytochrome C assay was used to monitor superoxide produced via the xanthine oxidase enzyme system. Superoxide ($O_2^{\cdot -}$) was generated with xanthine oxidase (10 nM) and xanthine (100 μM) in the presence of cytochrome c (50 μM) in PBS. To prevent interference from H_2O_2, 15 μg/mL catalase was added to the reaction. The reduction of cytochrome C by superoxide was monitored at 550 nm in the presence of different antioxidants to determine individual antioxidant activity. Besides iSODm, the antioxidants tested were: SODm, MnTBAP, and resveratrol, at concentration of 10 μM each.

Author Manuscript Author Manuscript Author Manuscript Author Manuscript

2.5 Immobilization of iSODm

iSODm immobilization is outlined in scheme 2. Glass coverslips or dummy silicon-based neural probes (A1X16-3mm-100) were submerged in a 1:1 MeOH:HCl solution for 30 minutes in a large crystallization dish with gentle agitation to remove organic residue. After rinsing with deionized water, concentrated H_2SO_4 was pipetted directly onto the samples. Following 30 minutes of acid surface activation, the samples were rinsed with deionized water and dried under N_2 flow overnight.

Pre-treated glass samples or silicon probes were submerged in a 2.5% solution of 3-mercaptopropyl trimethoxysilane (MTS) in toluene and shaken for 2 hours inside a glove bag under N_2. Afterwards, the samples were rinsed with copious amounts of toluene and sonicated in a water bath to remove excess unreacted silane. Sonicated samples were rinsed again with toluene and allowed to dry under N_2 flow. The heterobifunctional crosslinker N-ɣ-maleimidobutyryl-oxysulfosuccinimide ester (sulfo-GMBS) was dissolved in minimal amounts of DMF and diluted to 0.5 mg/mL in absolute ethanol. To activate the surface, the silanized surfaces were submerged in the sulfo-GMBS solution for 1 hour, then rinsed with absolute ethanol and dried. Finally, the functionalized iSODm complex was covalently attached to the activated surface by submerging the substrates in 1 mg/mL iSODm solution (PBS) for 1 hour. Successful coating was verified by confirmation of the reduction of silicon after iSODm coating and increase of manganese (iSODm) using X-ray photoelectron spectroscopy (XPS) for elemental composition with a MCL – ESCALAB 250 XI Thermo Scientific XPS (Supplementary Fig. S2).

2.6 *In vitro* bioactivity testing of iSODm immobilized surfaces

2.6.1 HAPI Cell Line—Frozen Highly Aggressive Proliferating Immortalized (HAPI) microglia cells [30] (provided by Dr. Xiaoming Hu, Department of Neurology, University of Pittsburgh) were thawed and passaged once before being plated at a density of 1×10^5 cells/cm^2 in 48-well plates. Cells to test the iSODm coating were plated directly onto glass coverslips that were coated with iSODm as described above. Cells to test the soluble antioxidants were plated directly onto glass coverslips in media containing either 10 μM Mn^{III}TE-2-Pyp5+(SODm), diphenyleneiodonium (DPI), MnTBAP, or resveratrol. Before activation, cells were grown until × 80% confluence (24 hours) in serum containing media [10% fetal bovine serum (FBS), Dulbecco's modified Eagle's media/F12 (DMEM/F12, Gibco 21041 DMEM/F12 +L-glutamine – HEPES – Phenol Red, Invitrogen, Carlsbad CA)]. Cells were plated in triplicate per group and incubated at 37 °C. Experiments were repeated 3 times to ensure reproducibility.

2.6.2 Inflammatory Activation of HAPI Cells—HAPI cells were incubated with stimulating agents to activate the immune response via either the damage-associated molecular pattern (DAMP) pathway or the pathogen-associated molecular pattern (PAMP) pathway. Following initial proliferation of cells, all cells were maintained in DMEM/F12 supplemented with 2% FBS and treatment conditions were replenished when changing media. For the PAMP pathway response, cells were stimulated with gram-negative bacteria-derived lipopolysaccharide (LPS, from Escherichia coli) at a concentration of 10 ng/mL in the presence of 2 ng/mL interferron gamma (IFNɣ) [31]. Cells were stimulated for 24h with

Author Manuscript Author Manuscript Author Manuscript Author Manuscript

LPS/IFNγ stimulation prior to measurement of oxidative species or fixation. DAMP pathway activation was triggered with incubation in serum-free media containing 50 ng/mL phobol 12-myristate 13-acetate (PMA) [32]. Cells were stimulated with PMA for 3 hours prior to the measurement of oxidative species or fixation.

2.6.3 Measurement of NO Output of Activated HAPI Cells—Nitric oxide production of stimulated cells was measured using the commercially available Griess reagent kit (Invitrogen, Carlsbad CA). Samples of the cellular supernatant were taken and mixed with the Griess reagent. Following 30 minutes of incubation at room temperature, NO levels were determined by measuring the absorbance at 540 nm. For each group, NO levels were normalized by cell count.

2.6.4 Measurement of $O_2^{\cdot -}$ Output of Activated HAPI Cells—Superoxide production by cells was monitored using the cytochrome C assay. In brief, 3 hours prior to the PMA stimulation endpoint, media containing 10 μM cytochrome C was added to each well. 3 hours after PMA stimulation, the reduction of cytochrome C was measured at 550 nm. For each group, $O_2^{\cdot -}$ levels were normalized by cell count.

2.6.5 Intracellular Staining of Reactive Oxygen Species—Intracellular staining of ROS was completed using the dihydrorhodamine (DHR dye. Prior to the endpoint for all conditions, media containing 10 μM DHR was added to each well. After 3 hours, cells were fixed with 4% paraformaldehyde and used for subsequent staining as described below.

2.6.6 In vitro Cell Staining, Imaging and Quantification—Immunofluorescence was performed on HAPI cells fixed with 4% paraformaldehyde (PFA) for 10 minutes and blocked with 10% goat serum for 45 minutes. The following monoclonal primary antibodies were incubated at room temperature together at a dilution of 1:500 for 1.5 hours in 2.5% goat serum in PBS: mouse anti-ED1 (AdD Serotec, Raleight NC), rabbit anti-iNOS (inducible nitric oxide synthase, Millipore), and chicken anti-arginase (arginase; Millipore). Cells previously stained with DHR (above) were incubated with rabbit anti-p47-phox (Millipore) for 1.5 hours. After washing, the appropriate fluorescence-conjugated secondary antibodies were added in 2.5% goat serum for 1.5 hours. Cell nuclei were counterstained with Hoechst 33258 2μg/mL; Sigma-Aldrich) at a dilution of 1:1000 in PBS. For a comparison of *in vitro* cell staining and DHR quantification, corrected total cell fluorescence (CTCF) was calculated. The intensity of cell bodies was measured using ImageJ, followed by subtraction of the background intensity, and then scaled to cell counts obtained by DAPI staining.

2.6.7 Primary Neuron Culture—The biocompatibility of the iSODm-coated surface was examined *in vitro* by primary rat neuronal cell cultures similar to methods described by Woeppel et. al. [33]. Neurons were harvested from E18 rat fetuses. Fetal brains were removed and digested in trypsin followed by trituration to produce a single cell suspension. The suspended cells were collected, centrifuged at 800 rpm for 10 minutes, then resuspended in neural basal media (Gibco) supplemented with 1% pen/strep (Invitrogen), 2% B27 (Gibco), and 1% GlutaMax (Gibco). Cells were plated over iSODm modified coverslips, poly-lysine modified coverslips, or bare glass and cultured for 48 hours at 37°C

Author Manuscript Author Manuscript Author Manuscript Author Manuscript

and 5% CO2. Poly-lysine coated coverslips were prepared by incubating 5 wt% aqueous poly-lysine (70kDa, Sigma) over cleaned glass coverslips for 1 hour. The supernatant was aspirated off and coverslips dried. Five samples were used per condition. After culture, cells were fixed in 4% paraformaldehyde in PBS then permeabilized in 0.2% triton-X. Neurons were stained for β-III-tubulin (Invitrogen) and DAPI (Invitrogen). Images were taken by Leica DMI 4000B fluorescence microscope. Three images were taken well and 5 well per sample. The culture was repeated three times.

2.6.8 In vitro evaluation of iSODm coating stability—To evaluate the antioxidant functionality of the coating, glass coverslips were coated with iSODm and soaked in pH 7.5 PBS at 37 °C in 5% CO_2 for 0, 3, 7, and 14 days (n = 5 coverslips for each soaking duration). Cytochrome C assay was performed at the end of the soaking test. Surface coating thickness was evaluated with ellipsometry, using a Cauchy model with a silicon substrate and absorbing film. Silicon wafers were coated with iSODm and soaked for 0, 3, 7, and 14 days in PBS at 37°C. Prior to measuring, samples were washed with excess DI-water, followed by drying under N_2 stream.

2.7 In vivo biocompatibility of iSODm Coated Neural Probes

All experiments and housing complied with the United states Department of Agriculture guidelines and were approved by the University of Pittsburgh's Institutional Animal Care and Use Committee. Non-functional A-style probes were implanted bilaterally in three adult male Sprague Dawley rats with a total of 9 control (uncoated) and 9 iSODm coated arrays. In each rat a total of 6 electrodes were implanted in the bilateral parietal cortex (3 electrodes implanted in each hemisphere, with at least 3 mm separation between implant sites). The surgeon was agnostic to the implant type and the implants were randomized such that there was no ipsilateral hemisphere bias for either coating condition. Two electrodes from each treatment either broke during manipulation or caused bleeding during implantation and were excluded from analyses leaving a total of 7 control (uncoated) and 7 (iSODm coated) arrays among three rats.

The rats were given general anesthesia with a mixture of 3% isoflurane in O_2 prior to implantation and were maintained at 1-2% isoflurane for the duration of the surgery. The state of anesthesia was closely monitored by observing the respiratory rate and the absence of the pedal reflex. The animal was placed in a stereotaxic frame and their head was shaven, disinfected with betadine followed by isopropyl alcohol three times, and a sterile drape was placed over the surgical area. Ophthalmic ointment was applied to the animal and the surface of the skull was exposed with a single incision along the midline. The surgeon was agnostic to the type of probe being implanted. Prior to insertion of the probes, the dura layer was removed using a 30-gauge needle bent at 90°. The probes were inserted manually using a stereotaxic frame with a vacuum inserter device that held the probes. Following implantation, the craniotomies were filled with Kwik-Sil (World Precision Instruments, Sarasota FL) followed by FUSIO liquid dental cement. The skin was sutured around the dental cement head-cap and the animals were allowed to recover.

Author Manuscript Author Manuscript Author Manuscript Author Manuscript

2.7.1 Immunohistochemistry of brain tissue—

After 1-week, animals were anesthetized with 50 mg/mL ketamine and 5 mg/mL xylazine administered via the intraperitoneal (IP) cavity with a dosage of 0.1 mL/100 g body weight. The animals were transcardially perfused with 4% (w/v) PFA in PBS. Prior to removing the probes from the brain, the skull was detached and post-fixed in PFA for 6 hours. The post-fixed brains were then equilibrated in 15% sucrose solution (4°C) overnight followed by 30% sucrose solution for an additional 24 hours until the tissue sank to the bottom of the sucrose vial The tissue was sectioned at a thickness of 25 μm after cryoprotection using optimal cutting temperature compound (OCT, Tissue-Tek, Torrance CA).

Tissue sections were hydrated in PBS and blocked with 10% normal goat serum. Following 45 minutes in 0.5% Triton X-100 in PBS, the sections were incubated with three groups of stains for sections that were 25 μm apart. Group 1 consisted of mouse monoclonal NeuN (Milipore MAB377 mouse 1:500), 4HNE (Abcam, ab46545, rabbit,1:250). Group 2 consisted of primary mouse NeuN, rabbit monoclonal caspase 3 (Cell Signaling, 9661S, 1:500), and IgG. Group 3 consisted of Iba-1 (Wako, NC9288364, rabbit, 1:500), iNOS (Milipore, 482728-100ul, rabbit, 1:500), and arginase (Milipore, ABS535, chicken, 1:1000). All sections were counterstained using Hoechst nuclear dye, cover-slipped and preserved with fluoromount-G (SouthernBiotech, OB100-01). The technician performing tissue staining was agnostic to the treatment groups.

2.8 Fluorescent Imaging and Quantitative Brain Tissue Analysis

Confocal fluorescent images were acquired using a FluoView 1000 (Olympus, Inc., Tokyo, Japan) at the Center for Biologic Imaging University of Pittsburgh. Images for each antibody were taken with the same laser power and the same photomultiplier tube voltages to reduce variability in image intensity. For *in vivo* images, all analyzed sections were from 450-950 μm depth. For each IHC stain, images of two to three sections were acquired and analyzed, resulting 14 to 16 sections for control sections, and 14 to 17 for iSODm coated sections (further details on sample size are provided in the captions for Fig 8-10). The density of neurons undergoing apoptosis was determined by counting neuron cell bodies co-labeled with NeuN and caspase-3 in concentric rings every 25 μm around the implant to 250 μm radially outwards. The total number of cells in each bin was counted using ImageJ *Cell Counter* plug in. M1 and M2 like macrophage was determined by counting cells that show co-expression of Iba1 and iNOS, and Iba1 and arginase, respectively[34], 4HNE, Iba1, and IgG were quantified using a custom intensity-based software [35]. Intensities of tissue sections of coated and uncoated groups were normalized to the intensity of an implant-free control location, at least 500 μm away from the implanted location. The researchers performing cell counting and intensity-based analyses were agnostic to the treatment groups.

2.9 Statistics

For comparisons between two groups, Student's *t*- test was used. This test was used to compare the difference in 4HNE intensity between 0-25 μm adjacent to the probe. For comparisons between more than two groups, one-way and two-way ANOVA with Tukey's post-hoc analysis was performed using MATLAB.

Author Manuscript Author Manuscript Author Manuscript Author Manuscript

3.0 Results

3.1 Design and Characterization of iSODm

The design of highly potent antioxidants is of great interest due to the role of oxidative species in cancer, neurologic disorders, and traumatic brain injury. We have designed an immobilizable antioxidant which retains the properties of Mn^{III}TE-2-Pyp^{5+} while presenting multiple amine groups for surface coupling. To demonstrate that the newly-synthesized iSODm maintains the properties that would make it an effective SODm, cyclic voltammetry (CV) was used to determine the redox potential of iSODm (Fig. 1(A)). The redox potential for iSODm was shown to be relatively unchanged from SODm at ~ 240 mV vs NHE, well within the catalytic window for superoxide dismutation.

To verify the superoxide scavenger activity of iSODm, the capacity of iSODm to remove superoxide in the xanthine and xanthine oxidase system was evaluated. The superoxide-mediated reduction of cytochrome C in the presence of several antioxidants including iSODm, $Mn^{III}TE\text{-}2\text{-}Pyp^{5+}$, MnTBAP, and resveratrol was measured (Fig 1(B)). Without any antioxidant treatment, cytochrome C reduction occurs at a constant rate indefinitely (PBS control). Likewise, the addition of resveratrol does not decrease the rate of cytochrome C reduction. MnTBAP's low $E_{1/2}$, is ineffective at preventing superoxide-mediated reduction of cytochrome C. Conversely, both $Mn^{III}TE\text{-}2\text{-}Pyp^{5+}$ and iSODm completely prevented cytochrome C reduction for the duration of the experiment.

3.2 Characterization of the iSODm coating

Immobilization of iSODm onto glass substrates was verified using water contact angle and ellipsometry. Changes in water contact angles between bare glass (47.5 ± 3.0), silanized glass (64.2 ± 3.2), GMBS functionalized glass (24.0 ± 4.0), and iSODm modified glass (33.9 ± 4.7) were all significant with $p<0.05$ (n=6, mean±SD). Coating thickness of the silane, GMBS, and iSODm modifications were measured at 10.6 ± 4.3, 2.6 ± 0.7, and 5.9 ± 2.3, respectively (n=6, mean±SD). X-ray photoelectron spectroscopy (XPS) was performed on glass coverslips coated and uncoated with iSODm to confirm the presence of Mn2p (Fig. S2). Stability of the coating was first demonstrated by submerging modified silicon wafers in PBS at 37°C for two weeks (Fig. S3), monitoring the coating thickness before soaking, and at 3, 7, and 14 days with ellipsometry. No significant in thickness was observed upon soaking and vigorous washing. To further verify that the superoxide scavenging ability of the coating persist, three groups of glass coverslips with and without coating were soaked for 0, 3, 7, and 14 days. At the end of the soaking experiment, a cytochrome C assay was performed on all coated substrates compared to negative (cytochrome C solution alone) and positive (cytochrome C in the presence of xanthine and xanthine oxidase) controls. The resulting cytochrome C absorbance (Fig. 1(C)) showed that coated coverslips soaked at 0, 3, 7 and 14 days effectively attenuated cytochrome C oxidation. To confirm that the coating does not compromise the electrical properties of the neural electrode sites, functional silicon neural electrodes were coated with iSODm and no significant change in electrical impedance was observed before and after coating (Fig. 1(D)).

Author Manuscript Author Manuscript Author Manuscript Author Manuscript

3.3 Effects of iSODm Coating in Microglia and Neuronal Cultures

To evaluate the antioxidant performance of the iSODm coating, an *in vitro* model was used based on the HAPI microglia cell line. Cells were either plated on glass (with or without various antioxidant treatment in media) or glass coverslips coated with the iSODm. Following stimulation of the cells to activate the inflammatory response, the oxidative output of the cells as well as the levels of several proteins important in ROS production were evaluated in all conditions. Following stimulation of HAPI cells with PMA, we observed over a 110% increase in cytochrome C reduction in control cells (Fig. 2(A)). Only cells plated on the iSODm coating or with SODm in solution approached pre-stimulation levels. MnTBAP showed the least effect among the Mn based antioxidants in suppressing superoxide production, which is to be expected as MnTBAP is not a superoxide scavenger and its primary action is to scavenge peroxynitrite [36, 37]. Following stimulation of HAPI cells on control glass with both PMA and LPS/ IFNγ, a significant increase in p47 staining is observed (Fig. 3). This increase is significantly reduced when cells are plated onto the iSODm coated substrates.

Lipopolysaccharide (LPS) is well-established as an effective stimulating agent to induce the inflammatory response of microglia [31] via the Pathogen-Associated Molecular Pattern (PAMP) pathway. Following activation by LPS/IFNγ, the activity of inducible nitric oxide synthase (iNOS) is increased resulting in production of nitric oxide. To measure NO production in cells stimulated with LPS/ IFNγ, the Griess reagent assay was used. Interestingly, both the cationic porphyrins (iSODm and SODm) as well as the anionic porphyrin MnTBAP resulted in significantly increased NO output as measured by the Griess assay (Fig. 2(B)). When looking at immunostaining for pro-inflammatory iNOS, the cells plated on both iSODm coated samples and control glass and stimulated by LPS/IFNγ showed higher levels of iNOS staining than the unstimulated counterparts. Meanwhile, a significantly lower iNOS expression after LPS/IFNγ was observed in wells with iSODm modified glass compared to the uncoated control (Fig. 4). The relative increase in NO output despite the lowered iNOS expression on the iSODm surfaces may be in part due to reduced NO breakdown. A primary breakdown mechanism of NO is via reacting with superoxide to form peroxynitrite [38]. Since the superoxide is scavenged by the iSODm, the NO breakdown is blocked leading to more NO. Another observation can be made when examining the Arg-1 staining. Both stimulations led to decreased levels of Arg-1 under most conditions, within the only modest increase observable for PMA stimulated cells on glass (Fig. 5).

The intracellular levels of superoxide were evaluated using the superoxide probe dihydrorhodamine (DHR) (Fig. 6). The non-fluorescent probe, DHR readily crosses the cell membrane; however, once it has reacted with superoxide it becomes the charged and fluorescent compound, rhodamine 123. When rhodamine 123 (Rho123) is produced via the reaction between DHR and superoxide in the cell, Rho123 can no longer leave the cell, enabling detection of intracellular superoxide levels. Microglia significantly increase in fluorescence following both PMA and LPS stimulation. However, when cells are plated on the iSODm coating, these intracellular levels of superoxide are abolished.

Author Manuscript Author Manuscript Author Manuscript Author Manuscript

To determine the effect of the iSODm coating on cell attachment and growth, we first examined the number of HAPI cells attached on uncoated or iSODm coated glass coverslips based on the nuclei stain. HAPI cell attachment decreased by 47% on the iSODm surfaces (83±24 cells per image, mean±SD) compared to the uncoated control (44±12 per image, mean±SD). Neuron attachment and outgrowth was also examined. Primary neurons were cultured on bare glass, iSODm modified glass, or control poly-lysine modified glass. As expected, neurons performed best when grown on the highly cationic poly-lysine surface, having significantly higher neurite outgrowth. While iSODm surface modifications lowered HAPI cell attachment, it promoted the neuron attachment and neurite extension compared to the bare glass. Neurons grown for 48h on iSODm coated substrates produced significantly more neurites than the uncoated samples (Fig. 7).

3.4 In Vivo Biocompatibility

To investigate *in vivo* biocompatibility of the coating, we implanted coated and uncoated dummy probes in the bilateral cortices of SD rats for 1 week. Fig. 8 shows immunohistochemistry of brain tissues with caspase-3 as a marker for cells under-going apoptosis. Fig. 8 (A,B) show representative images of tissue sections co-labeled with NeuN and caspase-3. NeuN cells that are co-labeled with caspase-3 were quantified in Fig. 8(C). There was a significant reduction in neurons undergoing apoptosis within 0-25μm of the iSODm coated probes compared to uncoated probes. 4-Hydroxynonenal (4HNE) is produced by lipid peroxidation in cells, and its activity increases during oxidative stress. The iSODm coated electrodes significantly reduced 4HNE activity between 0-25 μm adjacent to the implant compared to uncoated controls (Fig. 8 D-F). Additionally, the iSODm coated group showed significantly reduced IgG staining compared to uncoated controls (Fig. 9 A-C).

Fig. 10 (A-C) shows IBA1 microglia/macrophage activity, both implants elicited elevated IBA1 activity nearby; no statistical difference was detected between implant types. However, by co-labeling IBA-1 cells with iNOS, we observed a significant reduction in iNOS positive macrophage within the 0-25 μm of iSODm coated implants (Fig. 10, D-F). We did not observe a significant difference between the treatment groups for cells co-labeled with IBA-1 and arginase (Fig. 10, G-I).

4. Discussion

In the realm of synthetic antioxidants cationic metalloporphyrins such as $Mn^{III}TE\text{-}2\text{-}Pyp^{5+}$ have demonstrated some of the highest activity for superoxide scavenging [25]. The key characteristic of $Mn^{III}TE\text{-}2\text{-}Pyp^{5+}$ that makes it such an effective antioxidant is the complex's redox potential ($E_{1/2}$ = 230 mV vs NHE), which lies roughly half-way between the oxidation (−160 mV) and reduction (890 mV) potentials of superoxide. To be an effective superoxide dismutase mimic (SODm) and to catalytically dismutate superoxide, a metal complex must have a redox potential of ~ 200 - 350 mV. The anionic metalloporphyrin MnTBAP was initially believed to be an effective SODm and has been tested as a surface coating for neural implants [40]. However, combined with the complex's low $E_{1/2}$ which is nearly – 200 mV vs NHE, and the demonstration that impurities had bestowed earlier studies

Author Manuscript Author Manuscript Author Manuscript Author Manuscript

with SODm activity, research has determined MnTBAP to be an ineffective SODm [36]. In contrast, SODm $Mn^{III}TE\text{-}2\text{-}Pyp^{5+}$ has demonstrated extraordinarily high superoxide scavenging activity as well as antioxidant efficacy in several models of oxidative stress including *in vivo* models of stroke, diabetes, and cancer. Therefore $Mn^{III}TE\text{-}2\text{-}Pyp^{5+}$ is considered a better candidate for incorporation into an antioxidant coating [23] [24].

The antioxidant activity of the coatings was first measured through oxidation of the cytochrome-c assay in the absence of cells. In line with redox potentials gathered from CV, both our SODm and iSODm performed well in reducing or eliminating the reduction of cytochrome-c, while the MnTBAP had noticeably diminished effects. The antioxidant properties of resveratrol have been widely studied. However, unlike catalytic SOD complexes, the antioxidant properties of resveratrol are believed to occur via suppression of the NF-κB pathway following oxidative insult [41]. Therefore, its negligible impact on superoxide production in this non-biological assay is expected.

The effect of iSODm coating is then evaluated in the presence of microglia. One of the key mechanisms of the DAMP pathway is the activation of protein kinase C and subsequent phosphorylation/activation of the NADPH oxidase. Phorbol myristate acetate (PMA) has been shown to activate protein kinase C, resulting in superoxide production by microglia cells via NADPH oxidase [32], and was used to model superoxide production and inflammation according to the DAMP pathway. We examined the superoxide production and activity in the presence of SODm and the iSODm coating, in addition to antioxidants MnTBAP, resveratrol and ±. In choosing the testing concentration of all antioxidants, we considered that iSODm, as well as many other SODm, operate under a catalytic mechanism, regenerating the original compound. As such, lower concentrations are required for effective scavenging of equivalent concentrations of ROS. In addition, SODm has a strong light absorption, which makes colorimetric testing at higher SODm concentrations difficult. Therefore, we selected 10 μM due to the redox activity, minimal absorbance, and efficacy at doses lower than the published values of other anti-oxidants. DPI has been shown to decrease superoxide-mediated cytochrome c reduction following NADPH oxidase activation of primary mouse monocytes/macrophages via 12-*O*-Tetradecanoyl-13-acetate (TPA) [42]. However, literature has mixed results due to DPI's very broad effect on all flavoenzymes, and DPI has also been shown to raise superoxide concentrations in glia culture [43]. Here, we see minimal effects from DPI after stimulating cells with PMA, potentially due to competing factors causing increases and decreases in superoxide production. Resveratrol has also showed no significant effect on reducing superoxide concentration. This might be the result of a relatively low dose. While the control antioxidants were ineffective at blocking CytC reduction, the iSODm coating was found to significantly reduce superoxide level both extracellularly and intracellularly (DHR). This decrease in superoxide concentration is accompanied with increased expression of NADPH oxidase p47 and iNOS after activation relative to controls without antioxidants, confirming the antioxidant and anti-inflammatory potentials.

After LPS stimulation, both resveratrol and DPI were capable of lowering NO production. Interestingly, while the superoxide scavenging results show the antioxidant catalysis of SODm, NO production was increased. As shown in previous literature, with the presence of

Author Manuscript Author Manuscript Author Manuscript Author Manuscript

superoxide scavengers such as SOD, NO breakdown is drastically decreased resulting in overall higher levels [32]. Such finding is consistent with what has been found on iSODm surfaces. It is important to point out that, NO, in the absence of superoxide and subsequent peroxynitrite production, can be cytoprotective and important for angiogenesis [11].

While the main purpose of iSODm is to decrease the concentration of ROS, iSODm coatings show an additional benefit of supporting neural attachment and neurite outgrowth. This interaction may be encouraged by the amine groups presented by the iSODm molecule. While some amine groups are used for the binding of the iSODm to our substrates, the remaining amine groups result in a positively charged surface. This surface can act similarly to poly-lysine coated substrates, which is known to create positive charge, allowing for interactions with proteins, soluble peptides, and the polyanionic cell surface to encourage cell binding [44]. Examining the neurite outgrowth on iSODm vs. poly-lysine or uncoated coverslips, we observed that the antioxidant coated samples acted as an intermediate between the two. While this experiment did not directly examine the mechanism of cell outgrowth on iSODm coated substrates, it provided evidence that our modification is non-toxic and permissive to neural attachment and growth.

The *in vivo* biocompatibility results showed that iSODm coated probes significantly reduced 4HNE intensity immediately adjacent to the probe (0-25 μm). While the reduction in oxidative stress did not significantly alter neuron density (Supplemental Information, Fig. S4), the iSODm coating significantly reduced the number of neurons undergoing apoptosis and the number of pro-inflammatory macrophage/microglia cells. Furthermore, oxidative stress associates with BBB permeability alteration, specifically increases endothelium permeability to large molecules[45] [46, 47]. The BBB leakage is often indicated by stains of immunoglobulins (IgG), which is a blood protein not present in the brain tissue with intact BBB[48]. The reduction in IgG intensity immediately near the iSODm surface of the probe compared to the uncoated suggest that the reduction of oxidative stress prevented further breakdown of the blood brain barrier after the acute insertion damage. These results provide evidence that the coating was effective in reducing the negative consequences of oxidative stress immediately adjacent to the implant. It is important to note that the iSODm coating was only a monolayer on a smooth surface and can potentially only scavenge superoxide that react with the electrode surface, thereby affecting tissues within the 0-25 μm distance bin. However, our recent *in vitro* data has demonstrated that by increasing the functional surface area with a nanoparticle roughening strategy, we can amplify the antioxidant effect, potentially increasing the effective radius for *in vivo* applications [33]. We did not observe a statistical difference for arginase positive macrophage (M2-like) between the two groups. This may be attributed to the 1-week end-point, where the insertion injury was still in an acute stage and more proinflammatory macrophage (M1-like) are expected in high quantities[39].

5. Conclusion

We created a novel coating based on a newly synthesized superoxide dismutase mimic. By preparing an amine functionalized SODm derivative, a monolayer coating was created that demonstrated similar antioxidant effectiveness as $Mn^{III}TE\text{-}2\text{-}Pyp^{5+}$. Based on *in vitro*

Author Manuscript Author Manuscript Author Manuscript Author Manuscript

results, the iSODm coating effectively reduced superoxide production resulting in a decreased oxidative environment which ultimately affected HAPI cell signaling pathways by altering protein levels of iNOS and NADPH oxidase. Additionally, we have demonstrated coating efficacy under physiological conditions including reduced oxidative stress, neuronal apoptosis, BBB leakage and pro-inflammatory microglia/macrophage. Taken together, the iSODm coating showed great potential in alleviating tissue damage as a result of device insertion. Future work will investigate the effect of the iSODm coating for chronically implanted functional neural microelectrodes.

Supplementary Material

Refer to Web version on PubMed Central for supplementary material.

Acknowledgement

This project was financially supported by NIH NINDS Grant 5R01NS062019 and R01NS089688. The authors would like to thank University of Pittsburgh Center for Biologic Imaging for confocal microscopy and Dr. Joel Gillespie and Materials Characterization Laboratory at the Chemistry Department at the University of Pittsburgh for XPS.

8. Bibliography

[1]. Schwartz AB, Cui XT, Douglas J Weber DW Moran, Brain-Controlled Interfaces: Movement Restoration with Neural Prosthetics, Neuron 52(1) (2006) 205–220. [PubMed: 17015237]

[2]. Biran R, Martin DC, Tresco PA, Neuronal cell loss accompanies the brain tissue response to chronically implanted silicon microelectrode arrays, Exp Neurol 195(1) (2005) 115–26. [PubMed: 16045910]

[3]. Kozai TD, Eles JR, Vazquez AL, Cui XT, Two-photon imaging of chronically implanted neural electrodes: Sealing methods and new insights Journal of neuroscience methods 258 (2016) 46–55. [PubMed: 26526459]

[4]. Polikov VS, Tresco PA, Reichert WM, Response of brain tissue to chronically implanted neural electrodes, Journal of Neuroscience Methods 148(1) (2005) 1–18. [PubMed: 16198003]

[5]. Emerit J, Edeas M, Bricaire F, Neurodegenerative diseases and oxidative stress, Biomedicine & Pharmacotherapy 58(1) (2004) 39–46. [PubMed: 14739060]

[6]. Dexter D, Carter C, Agid F, Agid Y, Lees AJ, Jenner P, Marsden CD, Lipid peroxidation as cause of nigral cell death in Parkinson's disease, Lancet (London, England) 2(8507) (1986) 639–40.

[7]. Dexter DT, Carter CJ, Wells FR, Javoy-Agid F, Agid Y, Lees A, Jenner P, Marsden CD, Basal lipid peroxidation in substantia nigra is increased in Parkinson's disease, Journal of neurochemistry 52(2) (1989) 381–9. [PubMed: 2911023]

[8]. Gilgun-Sherki Y, Melamed E, Offen D, The role of oxidative stress in the pathogenesis of multiple sclerosis: the need for effective antioxidant therapy, Journal of neurology 251(3) (2004) 261–8. [PubMed: 15015004]

[9]. Gilgun-Sherki Y, Melamed E, Offen D, Antioxidant treatment in Alzheimer's disease: current state, Journal of molecular neuroscience : MN 21(1) (2003) 1–11. [PubMed: 14500988]

[10]. Piantadosi CA, Zhang J, Mitochondrial generation of reactive oxygen species after brain ischemia in the rat, Stroke; a journal of cerebral circulation 27(2) (1996) 327–31; discussion 332.

[11]. Brown GC, Neher JJ, Inflammatory neurodegeneration and mechanisms of microglial killing of neurons, Mol Neurobiol 41(2-3) (2010) 242–7. [PubMed: 20195798]

[12]. Block ML, Hong JS, Microglia and inflammation-mediated neurodegeneration: multiple triggers with a common mechanism, Prog Neurobiol 76(2) (2005) 77–98. [PubMed: 16081203]

Author Manuscript Author Manuscript Author Manuscript Author Manuscript

[13]. Lull ME, Block ML, Microglial activation and chronic neurodegeneration, Neurotherapeutics : the journal of the American Society for Experimental NeuroTherapeutics 7(4) (2010) 354–65. [PubMed: 20880500]

[14]. Kozai TDY, Li X, Bodily LM, Caparosa EM, Zenonos GA, Carlisle DL, Friedlander RM, Cui XT, Effects of caspase-1 knockout on chronic neural recording quality and longevity: Insight into cellular and molecular mechanisms of the reactive tissue response, Biomaterials 35(36) (2014) 9620–9634. [PubMed: 25176060]

[15]. George CM, Howard DR, Allan IL, Claire-Anne G, Robert EG, Ravi VB, Implanted neural electrodes cause chronic, local inflammation that is correlated with local neurodegeneration, Journal of Neural Engineering 6(5) (2009) 056003. [PubMed: 19700815]

[16]. Ereifej ES, Rial GM, Hermann JK, Smith CS, Meade SM, Rayyan JM, Chen K, Feng H, Capadona JR, Implantation of Neural Probes in the Brain Elicits Oxidative Stress, Frontiers in Bioengineering and Biotechnology 6(9) (2018).

[17]. Potter-Baker KA, Stewart WG, Tomaszewski WH, Wong CT, Meador WD, Ziats NP, Capadona JR, Implications of chronic daily anti-oxidant administration on the inflammatory response to intracortical microelectrodes, Journal of Neural Engineering 12(4) (2015) 046002. [PubMed: 26015427]

[18]. Prasad A, Sanchez JC, Quantifying long-term microelectrode array functionality using chronic in vivo impedance testing, Journal of Neural Engineering 9(2) (2012) 026028. [PubMed: 22442134]

[19]. Takmakov P, Ruda K Scott Phillips K, Isayeva IS, Krauthamer V, Welle CG, Rapid evaluation of the durability of cortical neural implants using accelerated aging with reactive oxygen species, J Neural Eng. 12(2) (2015)

[20]. Golabchi A, Wu B, Li X, Carlisle DL, Kozai TDY, Friedlander RM, Cui XT, Melatonin improves quality and longevity of chronic neural recording, Biomaterials 180 (2018) 225–239. [PubMed: 30053658]

[21]. Potter KA, Buck A, Self WK, Callanan ME, Sunil S, Capadona JR, The effect of resveratrol on neurodegeneration and blood brain barrier stability surrounding intracortical microelectrodes, Biomaterials. 34(29) (2013) 7001–15. [PubMed: 23791503]

[22]. Nguyen JK, Jorfi M, Buchanan KL, Park DJ, Foster EJ, Tyler DJ, Rowan SJ, Weder C, Capadona JR, Influence of resveratrol release on the tissue response to mechanically adaptive cortical implants, Acta Biomater 29 (2016) 81–93. [PubMed: 26553391]

[23]. Batinic-Haberle I, Reboucas JS, Spasojevic I Superoxide dismutase mimics: chemistry, pharmacology, and therapeutic potential, Antioxid Redox Signal 13(6) (2010) 877–918. [PubMed: 20095865]

[24]. Batinic-Haberle I, Spasojevic I, Tse HM, Tovmasyan A, Rajic Z, St Clair DK, Vujaskovic Z, Dewhirst MW, Piganelli JD, Design of Mn porphyrins for treating oxidative stress injuries and their redox-based regulation of cellular transcriptional activities, Amino acids 42(1) (2012) 95–113. [PubMed: 20473774]

[25]. Batinić-Haberle I, Manganese porphyrins and related compounds as mimics of superoxide dismutase, Methods in Enzymology, Academic Press2002, pp. 223–233.

[26]. Bernard AS, Giroud C, Ching HY, Meunier A, Ambike V, Amatore C, Collignon MG, Lemaitre F, Policar C, Evaluation of the anti-oxidant properties of a SOD-mimic Mn-complex in activated macrophages, Dalton Trans 41(21) (2012) 6399–403. [PubMed: 22407398]

[27]. Sompol P, Ittarat W, Tangpong J, Chen Y, Doubinskaia I, Batinic-Haberle I, Abdul HM, Butterfield DA, St Clair DK, A neuronal model of Alzheimer's disease: an insight into the mechanisms of oxidative stress-mediated mitochondrial injury, Neuroscience 153(1) (2008) 120–30. [PubMed: 18353561]

[28]. Mackensen GB, Patel M, Sheng H, Calvi CL, Batinic-Haberle I, Day BJ, Liang LP, Fridovich I, Crapo JD, Pearlstein RD, Warner DS, Neuroprotection from delayed postischemic administration of a metalloporphyrin catalytic antioxidant, J Neurosci 21(13) (2001) 4582–92. [PubMed: 11425886]

[29]. Kos I, Benov L, Spasojević I, Rebouças JS, Batinić-Haberle I, High lipophilicity of meta Mn(III) N-alkylpyridylporphyrin-based superoxide dismutase mimics compensates for their lower antioxidant potency and makes them as effective as ortho analogues in protecting superoxide

Author Manuscript Author Manuscript Author Manuscript Author Manuscript

dismutase-deficient Escherichia coli, J Med Chem 52(23) (2009) 7868–7872. [PubMed: 19954250]

[30]. Cheepsunthorn P, Radov L Menzies S, Reid J, Connor JR, Characterization of a novel brain-derived microglial cell line isolated from neonatal rat brain, Glia 31(1) (2001) 53–62.

[31]. Lee DC, Rizer J, Selenica M-LB, Reid P, Kraft C, Johnson A, Blair L, Gordon MN, Dickey CA, Morgan D, LPS- induced inflammation exacerbates phospho-tau pathology in rTg4510 mice, Journal of Neuroinflammation 7(1) (2010) 56. [PubMed: 20846376]

[32]. Bal-Price A, Matthias A, Brown GC, Stimulation of the NADPH oxidase in activated rat microglia removes nitric oxide but induces peroxynitrite production, Journal of neurochemistry 80(1) (2002) 73–80. [PubMed: 11796745]

[33]. Woeppel KM, Zheng XS, Cui XT, Enhancing surface immobilization of bioactive molecules via a silica nanoparticle based coating, Journal of Materials Chemistry B 6(19) (2018) 3058–3067. [PubMed: 30464839]

[34]. Orihuela R, McPherson CA, Harry GJ, Microglial M1/M2 polarization and metabolic states, Br J Pharmacol 173(4) (2016) 649–665. [PubMed: 25800044]

[35]. Kozai TDY, Gugel Z, Li X, Gilgunn PJ, Khilwani R, Ozdoganlar OB, Fedder GK, Weber DJ, Cui XT, Chronic tissue response to carboxymethyl cellulose based dissolvable insertion needle for ultra-small neural probes, Biomaterials 35(34) (2014) 9255–9268. [PubMed: 25128375]

[36]. Reboucas JS, Spasojevic I, Batinic-Haberle I, Pure manganese(III) 5,10,15,20-tetrakis(4-benzoic acid)porphyrin (MnTBAP) is not a superoxide dismutase mimic in aqueous systems: a case of structure-activity relationship as a watchdog mechanism in experimental therapeutics and biology, J Biol Inorg Chem 13(2) (2008) 289–302. [PubMed: 18046586]

[37]. Batinić-Haberle I, Cuzzocrea S, Rebouças JS, Ferrer-Sueta G, Mazzon E, Di Paola R, Radi R, Spasojević I, Benov L, Salvemini D, Pure MnTBAP selectively scavenges peroxynitrite over superoxide: Comparison of pure and commercial MnTBAP samples to MnTE-2-PyP in two models of oxidative stress injury, an SOD-specific Escherichia coli model and carrageenan-induced pleurisy, Free Radical Biology and Medicine 46(2) (2009) 192–201. [PubMed: 19007878]

[38]. Crow JP, Dichlorodihydrofluorescein and dihydrorhodamine 123 are sensitive indicators of peroxynitrite in vitro: implications for intracellular measurement of reactive nitrogen and oxygen species, Nitric oxide : biology and chemistry / official journal of the Nitric Oxide Society 1(2) (1997) 145–57.

[39]. Italiani P, Boraschi D, From Monocytes to M1/M2 Macrophages: Phenotypical vs. Functional Differentiation, Frontiers in immunology 5 (2014) 514–514. [PubMed: 25368618]

[40]. Potter-Baker KA, Nguyen JK, Kovach KM, Gitomer MM, Srail TW, Stewart WG, Skousen JL, Capadona JR, Development of superoxide dismutase mimetic surfaces to reduce accumulation of reactive oxygen species for neural interfacing applications, Journal of Materials Chemistry B 2(16) (2014) 2248–2258. [PubMed: 25132966]

[41]. Zhang F, Liu J, Shi J-S, Anti-inflammatory activities of resveratrol in the brain: Role of resveratrol in microglial activation, European Journal of Pharmacology 636(1–3) (2010) 1–7. [PubMed: 20361959]

[42]. Li Y, Trush MA, Diphenyleneiodonium, an NAD(P)H Oxidase Inhibitor, also Potently Inhibits Mitochondrial Reactive Oxygen Species Production, Biochemical and Biophysical Research Communications 253(2) (1998) 295–299. [PubMed: 9878531]

[43]. Riganti EGC, Polimeni M, Costamagna C, Bosia A and Ghigo D, Diphenyleneiodonium Inhibits the Cell Redox Metabolism and Induces Oxidative Stress, Journal of biological chemistry 273 (2004) 47726–47731.

[44]. Mazia D, Schatten G, Sale W, Adhesion of cells to surfaces coated with polylysine. Applications to electron microscopy, The Journal of Cell Biology 66(1) (1975) 198. [PubMed: 1095595]

[45]. Schreibelt G, Kooij G Reijerkerk A, Doorn R, Gringhuis SI, van der Pol S, Weksler BB, Romero IA, Couraud PO, Piontek J, Blasig IE, Dijkstra CD, Ronken E, de Vries HE, Reactive oxygen species alter brain endothelial tight junction dynamics via RhoA, PI3 kinase, and PKB signaling, FASEB J. 21(13) (2007) 3666–76. [PubMed: 17586731]

Author Manuscript Author Manuscript Author Manuscript Author Manuscript

[46]. Bennett C, Mohammed F, Álvarez-Ciara A, Nguyen MA, Dietrich WD, Rajguru SM, Streit WJ, Prasad A, Neuroinflammation, oxidative stress, and blood-brain barrier (BBB) disruption in acute Utah electrode array implants and the effect of deferoxamine as an iron chelator on acute foreign body response, Biomaterials 188 (2019) 144–159. [PubMed: 30343257]

[47]. Lochhead JJ, McCaffrey G, Quigley CE, Finch J, DeMarco KM, Nametz N, Davis TP, Oxidative stress increases blood-brain barrier permeability and induces alterations in occludin during hypoxia-reoxygenation, J Cereb Blood Flow Metab 30(9) (2010) 1625–1636. [PubMed: 20234382]

[48]. Nolta NF, Christensen MB, Crane PD, Skousen JL, Tresco PA, BBB leakage, astrogliosis, and tissue loss correlate with silicon microelectrode array recording performance, Biomaterials. 53 (2015) 753–62. [PubMed: 25890770]

Author Manuscript Author Manuscript Author Manuscript Author Manuscript

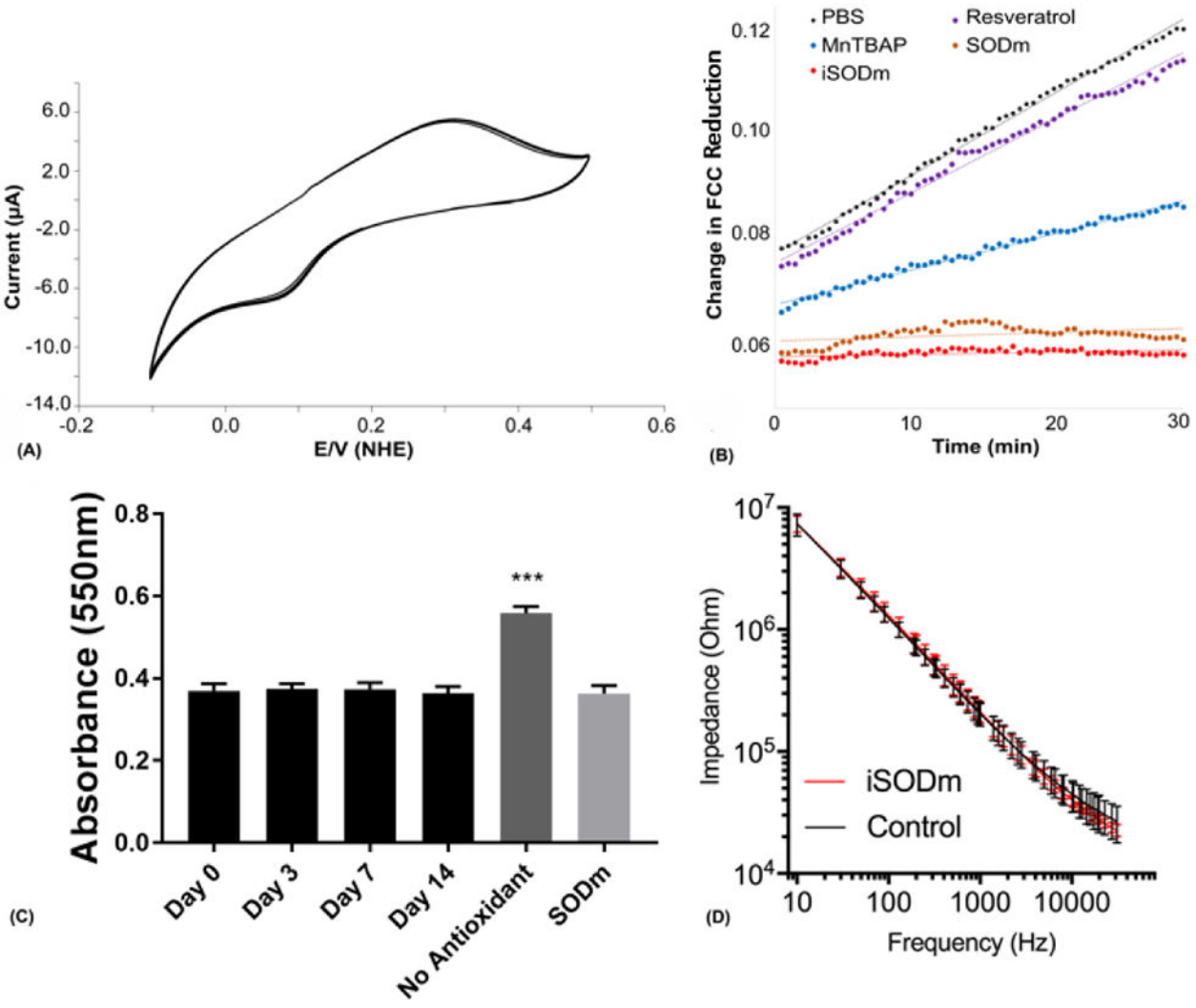

Figure 1.

(A) The cyclic voltammetry (CV) curve of iSODm at 100 mV/s in PBS vs. NHE. The $E_{1/2}$ of the synthesized iSODm is 220 mV vs. NHE, within the window necessary for catalytic dismutation of superoxide. **(B)** Antioxidant activity of iSODm compared to other known antioxidants. A constant supply of superoxide was generated using a xanthine oxidase/pterine enzymatic system. Superoxide concentration was measured using the ferricytochrome C (FCC) reduction assay. Only the cationic antioxidant SODm and the iSODm completely abolished FCC reduction indefinitely. **(C)** Antioxidant effect of the iSODm coating and in vitro stability. Coverslips coated with iSODm were soaked for 0, 3, 7, and 14 days. Cytochrome C assay performed at endpoint suggests stable iSODm coating for 2 weeks. All 4 soaking lengths resulted in a significant reduction in cytochrome C oxidation compared to the positive control (cytochrome C in the presence of xanthine and xanthine oxidase), n = 5, ***p< 0.001. No difference is detected between the soaked iSODm coverslips with the negative control (cytochrome C solution with soluble SODm). **(D)** Impedance spectroscopy for functional silicon probes with and without coating. The iSODm

Author Manuscript Author Manuscript Author Manuscript Author Manuscript

coating did not significantly change the electrical impedance of functional neural probes (n = 16 electrode sites for each condition).

Author Manuscript Author Manuscript Author Manuscript Author Manuscript

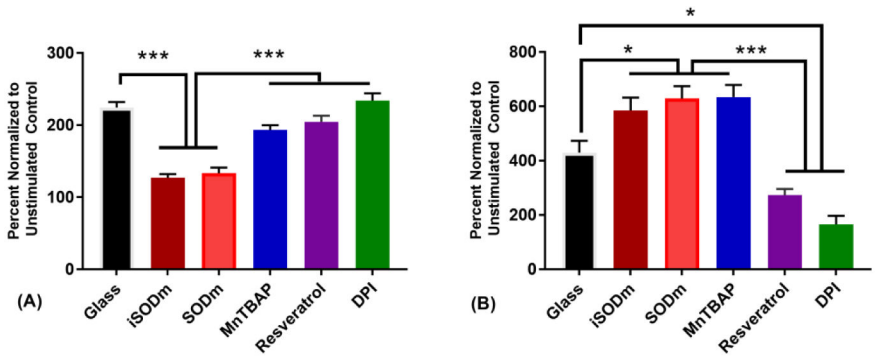

Figure 2.

(A) Superoxide production of PMA Stimulated HAPI cells measured by the FCC assay. FCC reduction by superoxide following PMA stimulation is completely abolished by both the iSODm coating and the SODm in solution (± SEM; $n = 9$; *** $p < 0.001$). **(B)** Griess Assay of LPS/IFNγ stimulated HAPI cells. Production of NO is only reduced with pre-treatment of the antioxidant resveratrol and DPI. All three metalloporphyrins result in a dramatic increase in measured NO (± SEM; $n = 9$; * $p < 0.05$, *** $p<0.001$).

Author Manuscript Author Manuscript Author Manuscript Author Manuscript

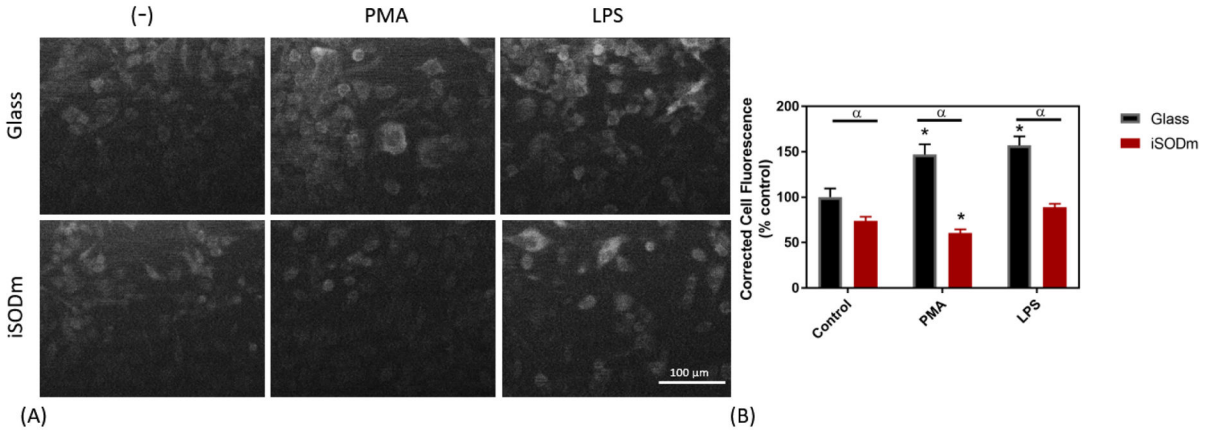

Figure 3.

Cellular levels of the NADPH oxidase protein, p47^{phox} in stimulated microglia cells. By using the corrected total cell fluorescence, a significant increase in p47 staining is observed in control microglia cells following treatment with either PMA or LPS. The CTCF from p47 staining is significantly lower in cells plated on the iSODm coating following PMA stimulation (± SEM; $n = 9$; * $p < 0.05$ compared to unstimulated glass control; α $p < 0.05$ between bare and iSODm coated glass).

Author Manuscript Author Manuscript Author Manuscript Author Manuscript

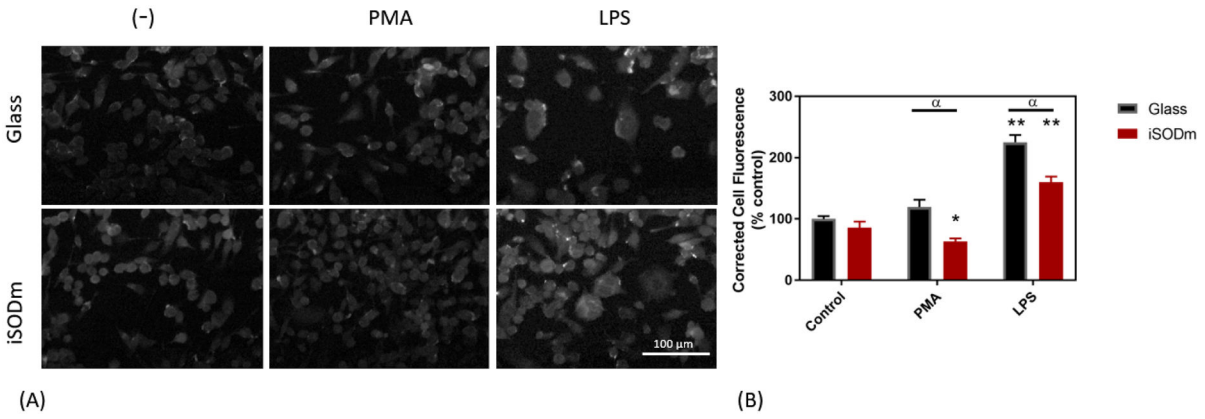

Figure 4.

Cellular staining of inducible nitric oxide synthase (iNOS) in stimulated microglia cells. Staining of iNOS is pronounced following LPS stimulation of microglia cells. The CTCF is significantly higher in microglia following LPS stimulation, and significantly increased further in cells plated on unmodified glass (± SEM; $n = 9$; * $p < 0.05$ compared to unstimulated glass control, α $p < 0.05$ between bare and iSODm coated glass).

Author Manuscript Author Manuscript Author Manuscript Author Manuscript

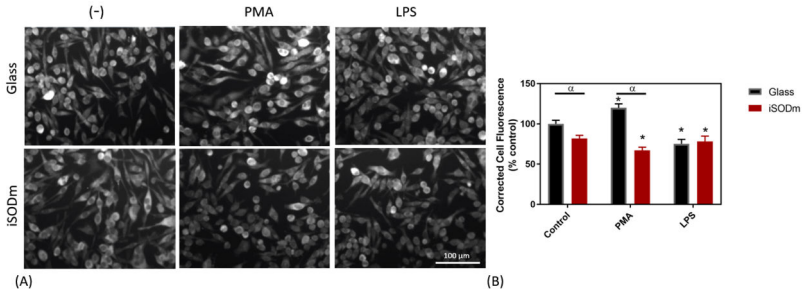

Figure 5.

Cellular staining of arginase protein in microglia cells. Arginase staining decreases upon stimulation of LPS in control microglia cells as measured by the CTCF but no significant difference was found between the bare and iSODm coated samples. However, PMA stimulation showed increase in arginase expression on glass and a decrease on iSODm (± SEM; $n = 9$; * $p < 0.05$ compared to unstimulated glass control; α $p < 0.05$ between bare and iSODm coated glass).

Author Manuscript Author Manuscript Author Manuscript Author Manuscript

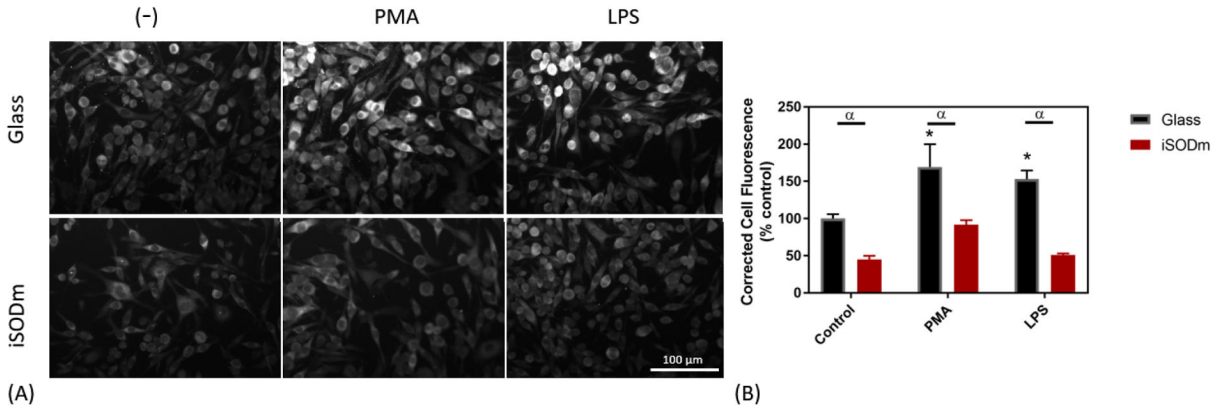

Figure 6.

Intracellular superoxide levels measured with dihydrorhodamine. Upon stimulation with either PMA or LPS, intracellular superoxide increases in microglia. In all cases, intracellular superoxide is decreased in cells grown on the iSODm coating (± SEM; $n = 9$; * $p < 0.05$ compared to unstimulated glass control; α $p < 0.05$ between bare and iSODm coated glass).

Author Manuscript Author Manuscript Author Manuscript Author Manuscript

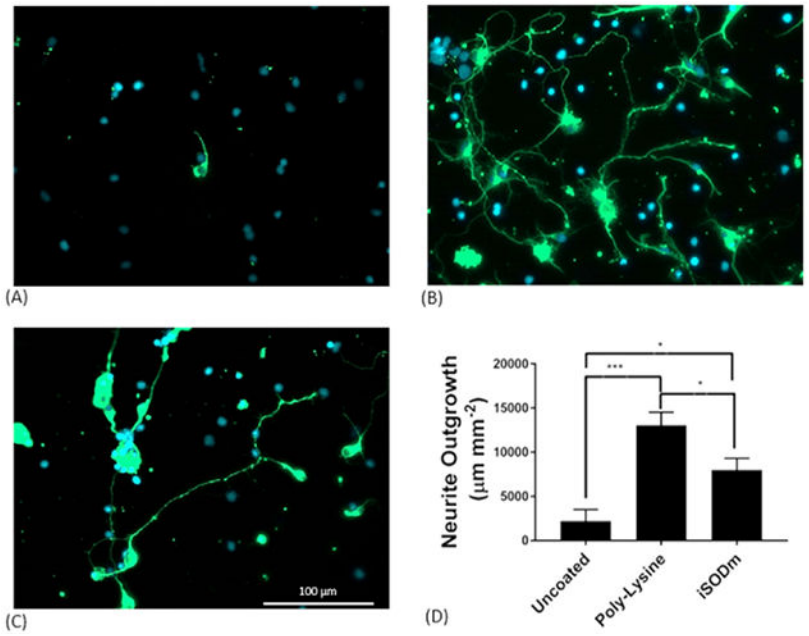

Figure 7.

The iSODm coating improves neuron growth and neurite extension. Primary neuron cultures grown on bare glass samples (A), samples coated with poly-lysine (B), or coated with iSODm (C). After 2 days, few cells are observed on uncoated glass samples while a high density of neurons (β-III tubulin, green) readily attach and grow on the poly-lysine and iSODm surfaces with healthy neurite outgrowth. A significant increase in outgrowth from the uncoated glass to the iSODm coated slides is observed. (*$p<0.05$, ***$p<0.001$)

Author Manuscript Author Manuscript Author Manuscript Author Manuscript

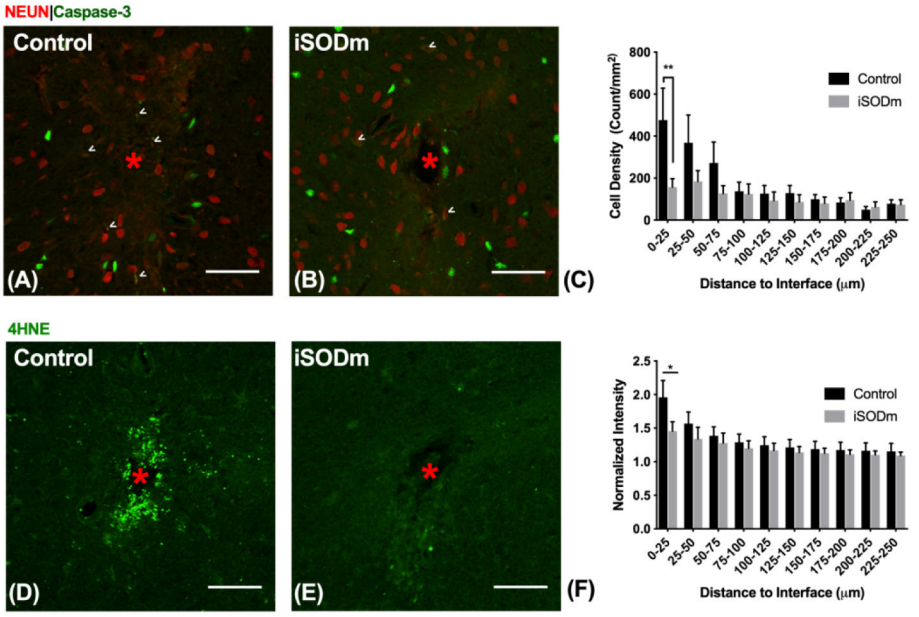

Figure 8.

Immunohistochemistry of brain tissue implanted with control and iSODm coated dummy probes. (A-C) Neuronal apoptosis. Neurons co-labeled with caspase-3 showed increased neuronal apoptosis near the implant (example cells indicated by white arrows), however, there was a significant reduction in apoptotic neurons near iSODm coated implant within 0-25 μm compared to control. (D-F) Oxidative stress (4HNE). Both implants showed elevated 4HNE expression immediately adjacent to the implant. However, iSODm coated electrodes significantly reduced overall 4HNE activity across all distance bins compared to control implants. n = 16 (control) n = 17 (iSODm) for each implant type; 2-3 repeated measures for each implant location (n = 7 locations for each implant type across N = 3 animals), $*p<0.05$. Error bars represent standard error of the mean. Scale bars represent 50 μm. Two-way ANOVA was used for comparisons in (C). Student's *t*-test was used for comparisons in (F) in the first distance bin.

Author Manuscript Author Manuscript Author Manuscript Author Manuscript

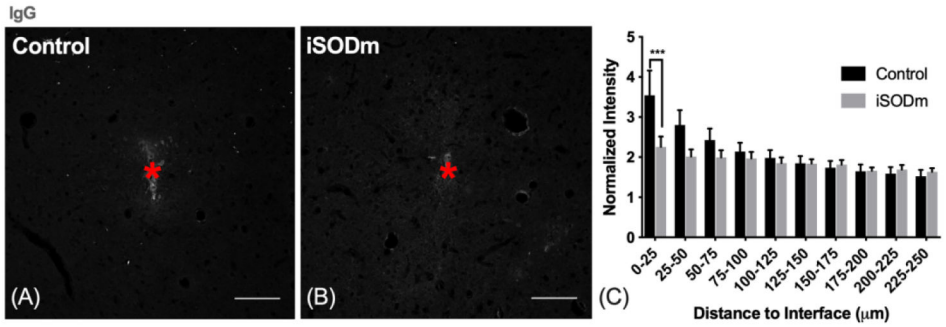

Figure 9.

(A-C) Blood brain barrier leakage. The presence of electrodes created BBB damage as indicated by higher intensity of IgG near both implants. However, at 0-25 μm away, iSODm coated probes elicited significantly less IgG compared to uncoated controls. ***$p < 0.001$. n = 16 (control) n = 17 (iSODm) sections for each implant type; 2-3 repeated measures for each implant location (n = 7 locations for each implant type across N = 3 animals). Error bars represent standard error of the mean. Scale bars represent 100 μm.

Author Manuscript Author Manuscript Author Manuscript Author Manuscript

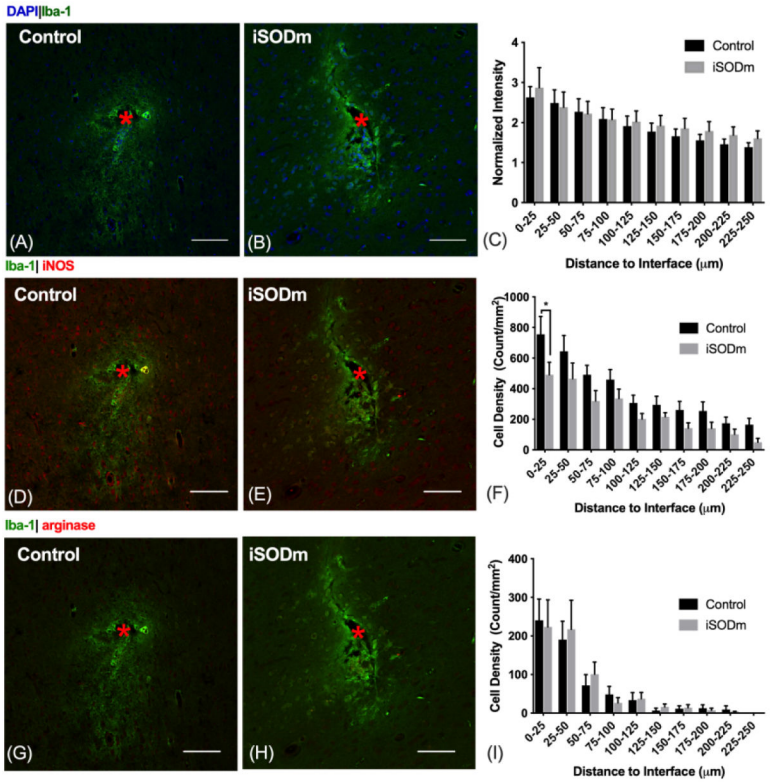

Figure10.

(A-C) Microglia/macrophage (IBA-1). The presence of implants elicited increased microglia and macrophage activity (IBA-1 intensity) at the probe vicinity with no statistical difference between the coated and the control probes. (D-F) M1-like macrophage. iNOS positive iba-1 cells showed higher aggregation around both types of implant. However, the density of these M1-like macrophage significantly reduced within the 0-25 μm bin for iSODm coated implants. *$p < 0.05$. (G-I) M2-like macrophages. Both implants elicited higher aggregation of M2-like macrophage near the implant with no statistical difference between implant types. n = 14 sections for each implant type; 2 repeated measures for each implant location (n = 7 locations for each implant type across N = 3 animals). Error bars represent standard error of the mean. Scale bars represent 100 μm.

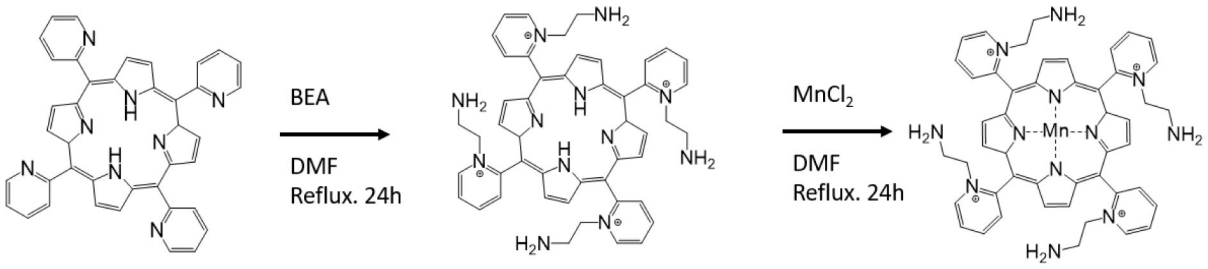

Scheme 1.
Reaction of H_2T-2-Pyp (meso-Tetra (2-pyridyl) porphine) to iSODm

Author Manuscript Author Manuscript Author Manuscript Author Manuscript

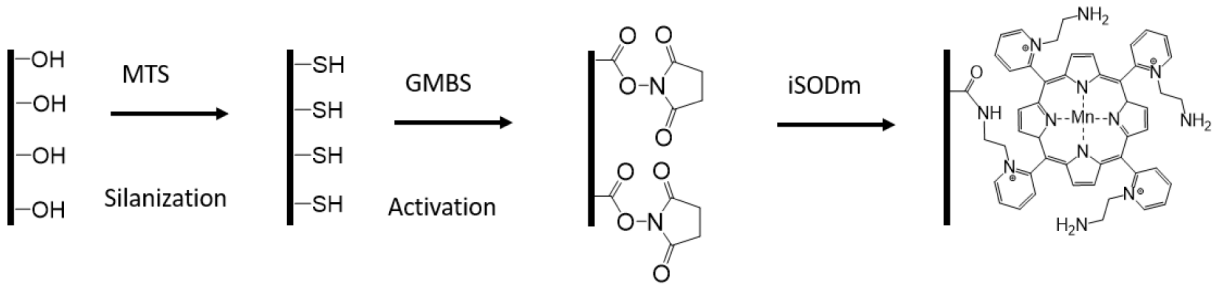

Scheme 2.
Immobilization of iSODm to substrates.

Author Manuscript Author Manuscript Author Manuscript Author Manuscript